An Adaptive Beamformer Algorithm-Based BMEVA Method for Enhanced Radar Imaging

René F. Vázquez Bautista[1], Luis J. Morales Mendoza[1], Andrés Blanco Ortega[2], and Francisco Beltrán Carbajal[3]

[1] Universidad Veracruzana, FIEC, Poza Rica, Veracruz, Mexico
favazquez@uv.mx, javmorales@uv.mx
[2] CENIDET Ingeniería Mecatrónica, Cuernavaca, Morelos, Mexico
andres.blanco@cenidet.edu.mx
[3] Universidad Politécnica de la Zona Metropolitana de Guadalajara, Tlajomulco de Zúñiga, Jalisco, Mexico
francisco.beltran@upjal.edu.mx

Abstract. In this paper, an adaptive beamformer algorithm LMS is presented and showed to improve the Bayesian Maximum Entropy–Variational Analysis (BMEVA) performance for high resolution radar imaging and denoising. A formalism to fuse the BMEVA and its integration inside the LMS structure is also presented. Finally, the image enhancement and denoising produced by the proposed Adaptive BMEVA method is analyzed, and the filter computational performance is demonstrated via SAR images scenarios.

Keywords. Data fusion, adaptive filter, LMS, SAR images, Bayesian maximum entropy.

Método BMEVA para formación mejorada de imágenes de radar basado en el algoritmo formador de haz adaptivo

Resumen. En este artículo se presenta la aplicación del algoritmo formador de haz adaptivo: Mínimos Cuadrados Medios (LMS), para mejorar el desempeño del método fusionado Máxima Entropía Bayesiana con Análisis Variacional (BMEVA) para formación de imágenes de radar de alta resolución y reducción del ruido. Además, el formalismo para integrar el método BMEVA fusionado, así como la inclusión bajo la estructura del LMS, es presentado. Finalmente, el mejoramiento de la imagen y la reducción del ruido producido por el método Adaptivo BMEVA es analizado, así como el desempeño computacional del filtro en función del IOSNR a través de diferentes escenarios con imágenes de Radar de Apertura Sintética.

Palabras clave. Fusión de datos, filtrado adaptivo, LMS, imágenes SAR, máxima entropía bayesiana.

1 Introduction

Recently, the Bayesian maximum entropy (BME) method was developed in [10], where the Bayesian estimation method for high resolution radar image formation [6, 4] employs the maximum entropy (ME) information theoretical-based windowing of the resulting images. Moreover, an alternative approach to radar image enhancement and denoising was proposed in [3] where the variational analysis (VA) paradigm was applied in [1, 5] to control the image gradient flow over the sensing scene using the difference-form approximations of the partial differential equations (PDE) to formalize different image processing problems including image segmentation, enhancement and denoising [3, 11, 2]. This strategy is adapted for a particular remote sensing system model and a priori robust information about the noise statistics and the desired image. The BME is associated in [10], [11, 13] with the spatial spectrum pattern (SSP) of the wavefield backscattered from the probing surface. As the SSP represents the power distribution in the RS environment, the power non-negativity constraint is incorporated implicitly in the BME strategy but specific VA geometrical properties of the image, e.g. its gradient flow over the scene/frame [5], are not incorporated. However, the so-called data fusion [12] strategy is a useful way to aggregate the BME statistical approach to optimize the VA-based radar image enhancement using a priori information [13]. The

fused BMEVA approach in [14] is presented and developed into a robust formalism without an efficient computational performance. However, recently, several efforts have been directed toward the high performance computing because of the computational load and implementation represents critical problem [9]. The latter produces the problem of finding a way to include the BMEVA method for performing the combined statistical-descriptive enhancement of the radar images based on adaptive algorithm.

2 Inverse Problem Statement

Based on [10], we define the model of the observation wavefield *u* by specifying the stochastic equation of observation of an operator form $u = Se + n$; $e \in \mathbf{E}$; $u, n \in \mathbf{U}$; S: $\mathrm{E} \rightarrow \mathrm{U}$, in Hilbert signal spaces E and U with the metrics structures induced by the inner products, $[u_1, u_2]_{\mathrm{U}}$ and $[e_1, e_2]_{\mathrm{E}}$, respectively, where the Gaussian zero-mean random fields *e, n,* and *u* correspond to the initial scattered field, noise and observation wavefield, respectively. Now, recalling the experiment design (ED) theory-based projection formalism [10], one can proceed from the operator form equation of observation to its finite-dimensional vector form,

$$\mathrm{U}=\mathrm{SE}+\mathrm{N} \tag{1}$$

where **E**, **N**, and **U** represent the zero-mean Gaussian vectors with the correlation matrices $\mathbf{R}_E=\mathbf{R}_E(\mathbf{B})$ = diag{**B**}, $\mathbf{R}_N$,and $\mathbf{R}_U = \mathbf{S}\mathbf{R}_E\mathbf{S}^+ + \mathbf{R}_N$, respectively, where diag{**B**} is a diagonal *K*-by-*K* matrix with elements $B_k = \langle E_k E_k^* \rangle$ and $\langle\cdot\rangle$ defines the statistical averaging operator. Vector **B** is referred to as the spatial spectrum pattern (SSP) vector that represents the average brightness image of the remotely sensed scene, and matrix **S** defines the signal formation operator (SFO).

3 Bayesian Maximum Entropy and Variational Analysis

3.1 BME Analysis

The processing of the observation data **U** is used to obtain a unique and stable estimate $\hat{\mathbf{B}}$. However, because of the ill-posed nature of such the image reconstruction problem [10], the SFO, in general, is ill-conditioned or even singular. Following the ME approach in [7], the a priori pdf $p(\mathbf{B})$ of the desired image is defined via maximization of the entropy of the image probability that also satisfies the constraints imposed by the prior knowledge [10]. The vector **B** is viewed as an element of the *K*-D vector space $\mathrm{B}_{(K)} \ni \mathbf{B}$ with the squared norm imposed by the inner product $\|\mathbf{B}\|^2_{B(K)} = [\mathbf{B},\mathbf{MB}]$, where **M** is the positive definite metrics inducing matrix [10]. In addition, the physical factors of the experiment can be generalized imposing the physically obvious constraint bounding the average squared norm of the SSP [10],

$$\int_{\mathbf{B}_C} [\mathbf{B},\mathbf{MB}]\, p(\mathbf{B})\, d\mathbf{B} \le c_{\mathrm{O}} \tag{2}$$

Thus, the a priori pdf $p(\mathbf{B})$ is to be found as a solution to the Lagrange maximization problem, with the Lagrange multipliers α, and λ. This problem is specified by the expression

$$\begin{aligned} -\int_{\mathbf{B}_C} \ln p(\mathbf{B})\, p(\mathbf{B})\, d\mathbf{B} - \alpha\Big(\int_{\mathbf{B}_C} [\mathbf{B},\mathbf{MB}]\, p(\mathbf{B})\, d\mathbf{B} - c_0\Big) \\ - \lambda\Big(\int_{\mathbf{B}_C} p(\mathbf{B})\, d\mathbf{B} - 1\Big) \rightarrow \max_{p(\mathbf{B})} \end{aligned} \tag{3}$$

for $\mathbf{B} \in B_C$, and $p(\mathbf{B}) = 0$ otherwise. The solution to (3) was derived in [10] that yields the Gibbs-type a priori pdf

$$p(\mathbf{B} \mid \alpha) = \exp\{-\ln \textstyle\sum(\alpha) - \alpha[\mathbf{B},\mathbf{MB}]\} \tag{4}$$

where $\sum(\alpha)$ represents the so-called Boltzmann statistical sum [10]. The log-likelihood [10] of the vector **B** is defined as

$$\Lambda(\mathbf{B}\,|\,\mathbf{U}) = \ln p(\mathbf{B}\,|\,\mathbf{U}) = -\ln\det\{\mathbf{SD}(\mathbf{B})\mathbf{S}^{+} + \mathbf{R}_{\mathbf{N}}\} - [\mathbf{U},(\mathbf{SD}(\mathbf{B})\mathbf{S}^{+} + \mathbf{R}_{\mathbf{N}})^{-1}\mathbf{U}] \tag{5}$$

and BME strategy for image reconstruction (estimation of the SSP vector **B**) is stated as

$$\hat{\mathbf{B}} = \arg\min_{\mathbf{B},\alpha}\{-\Lambda(\mathbf{B}\,|\,\mathbf{U}) - \ln p(\mathbf{B}\,|\,\alpha)\} \tag{6}$$

The BME estimate of the SSP is a solution to the problem (6) and is given by the nonlinear equation [10]

$$\hat{\mathbf{B}} = \mathbf{W}(\hat{\mathbf{B}})[\,\mathbf{V}(\hat{\mathbf{B}}) - \mathbf{Z}(\hat{\mathbf{B}})\,] \tag{7}$$

Here, $\mathbf{V}(\hat{\mathbf{B}}) = \{\mathbf{F}(\hat{\mathbf{B}})\mathbf{U}\mathbf{U}^{+}\mathbf{F}^{+}(\hat{\mathbf{B}})\}_{\text{diag}}$ is a vector that has the statistical meaning of a sufficient statistics (SS) for the SSP estimator, the operator $\mathbf{F}(\hat{\mathbf{B}}) = \mathbf{D}(\hat{\mathbf{B}})(\mathbf{I}+\mathbf{S}^{+}\mathbf{R}^{-1}_{\mathbf{N}}\mathbf{S}\mathbf{D}(\hat{\mathbf{B}}))^{-1}\mathbf{S}^{+}\mathbf{R}^{-1}_{\mathbf{N}}$ is referred to as the SS formation operator, the vector $\mathbf{Z}(\hat{\mathbf{B}}) = \{\mathbf{F}(\hat{\mathbf{B}})\mathbf{R}_{\mathbf{N}}\mathbf{F}^{+}(\hat{\mathbf{B}})\}_{\text{diag}}$ is the shift or bias vector, and $\mathbf{W}(\hat{\mathbf{B}}) = (\mathbf{T}(\hat{\mathbf{B}})+2\,\hat{\alpha}\,\mathbf{D}^{2}(\hat{\mathbf{B}})\mathbf{M})^{-1}$ has the statistical meaning of a solution dependent (i.e., adaptive) window operator with the stabilizer $\mathbf{T}(\hat{\mathbf{B}}) = \text{diag}\{\{\mathbf{S}^{+}\mathbf{F}^{+}(\hat{\mathbf{B}})\mathbf{F}(\hat{\mathbf{B}})\mathbf{S}\}_{\text{diag}}\}$.

3.2 Variational Analysis

Now, looking for a statistical interpretation of the Perona-Malik [1] anisotropic diffusion equation, it is possible to make the robustification of the VA-based image model. The generalized robustified VA energy function is defined in [3] as

$$VA(\mathbf{B}) = \int_{\Omega}\rho(||\nabla\mathbf{B}||)\,d\Omega \tag{8}$$

over the image domain Ω, where

$$\rho(x) = \int g(x)x\,dx = \sigma^{2}\log\left[1+\frac{1}{2}\left(x^{2}/\sigma^{2}\right)\right] \tag{9}$$

is the Lorentz function, and

$$g(x) = \rho'(x)/x \tag{10}$$

is the auxiliary function that defines the relation between the different reconstructed images after applying the robust VA estimation method [1].

The VA approach assumes the minimization of (8) via gradient descendent flow using the calculus of variations as follows:

$$VA(\hat{\mathbf{B}}) = \arg\min_{\mathbf{B}}\int_{\Omega}\rho(||\nabla\mathbf{B}||)\,d\Omega \tag{11}$$

In such a VA approach, the critical issue is the choice of the variational functional. Recall that in this study we follow the Lagrangian model given by (8).

4 Inverse Problem Statement

The fused BMEVA method for image reconstruction presented in [13] combines the VA and BME approaches and the formalism used the following strategies:

$$\hat{\mathbf{B}} = \arg\min_{\mathbf{B},\alpha}\{-\Lambda(\mathbf{B}\,|\,\mathbf{U}) - \ln p(\mathbf{B}\,|\,\alpha)\} \tag{12}$$

$$VA(\hat{\mathbf{B}}) = \arg\min_{\mathbf{B}}\int_{\Omega}\rho(\,||\nabla\mathbf{B}||)\,d\Omega \tag{13}$$

It is important to understand that both the BME and VA approaches look for an enhanced reconstruction with edge preservation. Henceforth, the proposed fused BMEVA reconstruction strategy assumes the solution to the variational problem:

$$\hat{\mathbf{B}}_{BMEVA} = \arg\min_{\mathbf{B},\alpha}\{-\Lambda(\mathbf{B}\,|\,\mathbf{U}) - \ln p(\mathbf{B}\,|\,\alpha) + \int_{\Omega}\rho(||\nabla\mathbf{B}||)\,d\Omega\} \tag{14}$$

The logarithm series expression is a viable mathematical tool to obtain the numerical approximation from the energy function by series. Recalling [13], the conventional gradient method is used to solve (14), as follows:

$$\sigma^2 \log\left[1+\left(\frac{||\nabla \mathbf{B}||}{\sigma\sqrt{2}}\right)^2\right] = \sigma^2 \sum_{n=1}^{2} \frac{(-1)^{n+1}\left(\frac{||\nabla \mathbf{B}||}{\sigma\sqrt{2}}\right)^{2n}}{n} = \mathbf{B}^{+}\mathbf{Q}\mathbf{B} \quad (15)$$

where

$$\mathbf{Q} = (1/2)\mathbf{L} + \tau_1 \mathbf{L}\mathbf{L} + \tau_2 \mathbf{L}\mathbf{L}\mathbf{L} \quad (16)$$

is the composed weighting matrix and the regularization parameters are τ_1= -1/8σ^2 and τ_2=1/24σ^4, respectively. The new proposed weighting matrix (16) was obtained using the consideration, *n*=3. The matrix **L** represents the numerical approximation of the Laplacian operator [11]. Now, the solution to the problem (14) can be expressed in the form of a nonlinear equation

$$\begin{aligned} F(\mathbf{B},\alpha) &= \ln\det\{\mathbf{S}\mathbf{D}(\mathbf{B})\mathbf{S}^{+} + \mathbf{R}_{\mathbf{N}}\} \\ &+ [\mathbf{U},(\mathbf{S}\mathbf{D}(\mathbf{B})\mathbf{S}^{+} + \mathbf{R}_{\mathbf{N}})^{-1}\mathbf{U}] \\ &+ \ln\sum(\alpha) + \alpha[\mathbf{B},\mathbf{M}\mathbf{B}] + [\mathbf{B},\mathbf{Q}\,\mathbf{B}]. \end{aligned} \quad (17)$$

$$\partial F(\mathbf{B},\alpha)/\partial \mathbf{B} = 0 \quad \text{and} \quad \partial F(\mathbf{B},\alpha)/\partial \alpha = 0 \quad (18)$$

As it was specified in [10], no unique regular method for solving (18) exists because of nonlinearity. However, one can represent the solution in a form convenient for further analysis. Finally, to proceed in this direction, we follow the methodology proposed in [10] which yields the following solution:

$$\hat{\mathbf{B}} = \mathbf{W}(\hat{\mathbf{B}})[\,\mathbf{V}(\hat{\mathbf{B}}) - \mathbf{Z}(\hat{\mathbf{B}})\,] \quad (19)$$

where

$$\mathbf{W}(\hat{\mathbf{B}}) = (\mathbf{T}(\hat{\mathbf{B}}) + 2\hat{\alpha}\mathbf{D}^2(\hat{\mathbf{B}})\mathbf{M} + 2\mathbf{Q})^{-1} \quad (20)$$

represents the spatial window operator.

5 The Adaptive Beamformer Algorithm

The derived BMEVA estimator (19) can be converted into an efficient iterative algorithm to adjust the spatial window operator coefficients on (20), according to the received array data to achieve an adaptive approach to the specified scenario. This adaptive beamforming structure considers a reference signal to minimize the cost function based on the signal´s mean square error (MSE), ε=$||B_k - \hat{B}_k||^2$. Then, the LMS algorithm is invoked to tackle the adaptive beamforming module, as follows:

$$\mathbf{W}(\hat{\mathbf{B}})^{(t+1)} = \mathbf{W}(\hat{\mathbf{B}})^{(t)} + \gamma[\mathbf{P} - \mathbf{R}_{\mathbf{E}}(\hat{\mathbf{B}})\,\mathbf{W}(\hat{\mathbf{B}})^{(t)}], \quad (21)$$

where, **P**=< **U***B_k^* >, which leads directly to the least mean square algorithm [2]:

$$\mathbf{W}(\hat{\mathbf{B}})^{(t+1)} = \mathbf{W}(\hat{\mathbf{B}})^{(t)} + \gamma[\varepsilon^{*(t)} * \mathbf{U}^{(t)}] \quad (22)$$

Pursuing such an approach, we refer to the SSP estimate on the right-hand side in (19) as the current estimate $\mathbf{W}(\hat{\mathbf{B}})^{(t)}$ at the *t*-th iteration step, and associate the entire right-hand side of (19) with the rule for forming the estimate $\mathbf{W}(\hat{\mathbf{B}})^{(t+1)}$ for the next iteration step (*t*+1) that yields. Due to the performed regularized windowing (20), the iterative algorithm (22) converges in a polynomial time regardless of the choice of the balance factor γ within the prescribed normalization interval, 0≤γ≤1. Moreover, the convergence and stability of the LMS algorithm depend on the factor γ. If γ is small, adaptation is slow but the excess mean square error after adaptation is small.

6 Simulations

In this section, virtual simulations are presented based on the Synthetic Aperture Radar (SAR) systems, that are related to the Point Spread Function (PSF), e.g., Gaussian (system 1), and Sinc (system 2). These PSF represent particular SAR system to compute the Adaptive Algorithm under study. Figure 1 shows the simulated scene **B** and the computed results produced by the Match Spatial Filter (MSF), VA method, BMEVA method, in Figures 1.b-1.d, respectively. In addition, Figure 1.e, and Figure 1.f, present the ABMEVA enhanced imaging reconstruction and the improved identification is clearly seen. The scenes used in these simulations impose image

reconstruction challenges because the scenes include textures, edges, and clustered zones. Moreover, the radar imagery showed in Figure 1 and Figure 3 are based on Gaussian-type PSF. However, the factor γ was applied inside the normalized restriction to guarantee the stability through the new adaptive algorithm (24). On the other hand, Figure 2 and 4 show the results of the image enhancement using the sin(*ax*)/*ax*, i.e., sinc-type PSF. Figure 4 is composed by the reconstructed radar images via the family of algorithms previously reported in Table 2. However, both Figure 3 and Figure 4, show the results through a different radar scene (**B'**) with edges and flat zones clearly defined. The iterative algorithm used to evaluate the sub-optimal ABMEVA approach was conditioned to $\varepsilon \leq 5e^{-8}$. Hence, Table 1 presents clearly the IOSNR-based quantitative evaluation for the first scene oriented to sharp edges and to distinguish zones. However, the qualitative viewpoint is a critical reference to make decision because the zones are close. On the other hand, Table 2 describes the IOSNR-based quantitative evaluation for the second scene oriented to sharp edges and to preserve flat zones. Once again, the qualitative perspective supports the ABMEVA-based outstanding enhanced radar imaging. Finally, Table 1 and the Table 2 present the quantitative analysis that confirms the ABMEVA computational performance based on input-output signal-noise ratio (IOSNR) metric.

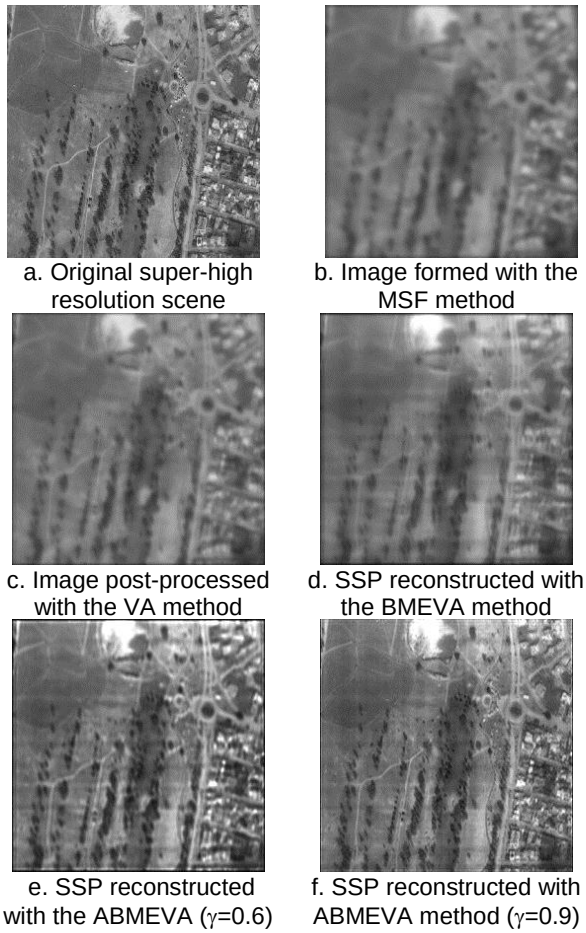

a. Original super-high resolution scene
b. Image formed with the MSF method
c. Image post-processed with the VA method
d. SSP reconstructed with the BMEVA method
e. SSP reconstructed with the ABMEVA (γ=0.6)
f. SSP reconstructed with ABMEVA method (γ=0.9)

Fig. 1. Simulation for **B** scene (1st system model)

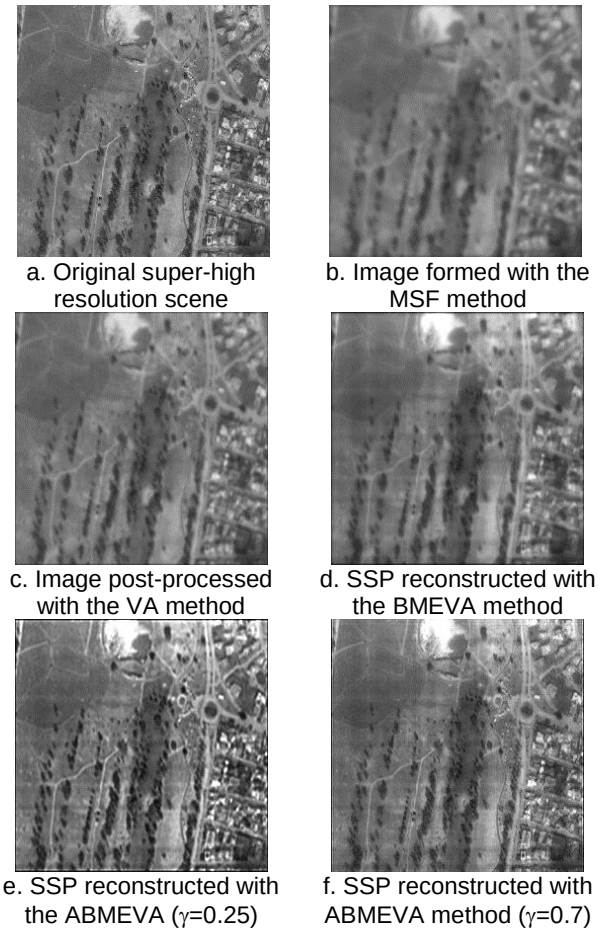

a. Original super-high resolution scene
b. Image formed with the MSF method
c. Image post-processed with the VA method
d. SSP reconstructed with the BMEVA method
e. SSP reconstructed with the ABMEVA (γ=0.25)
f. SSP reconstructed with ABMEVA method (γ=0.7)

Fig. 2. Simulation for **B** scene (2nd system model)

Table 1. Scene **B**-based results for two different simulated SAR systems

SNR [dB]	*IOSNR* [dB] System 1 Reconstruction Method				*IOSNR* [dB] System 2 Reconstruction Method			
μ	*VA*	*BMEVA*	*ABMEVA* (γ=0.6)	*ABMEVA* (γ=0.9)	*VA*	*BMEVA*	*ABMEVA* (γ=0.25)	*ABMEVA* (γ=0.7)
10	0.635	2.12	8.301	9.711	1.335	3.025	11.926	13.575
15	0.638	2.625	8.322	9.753	1.351	3.128	11.941	13.581
20	0.638	3.142	8.354	9.773	1.356	4.335	11.978	13.59
25	0.64	4.43	8.369	9.781	1.358	5.498	11.982	13.603
30	0.642	4.732	8.375	9.8	1.36	6.133	11.993	13.615

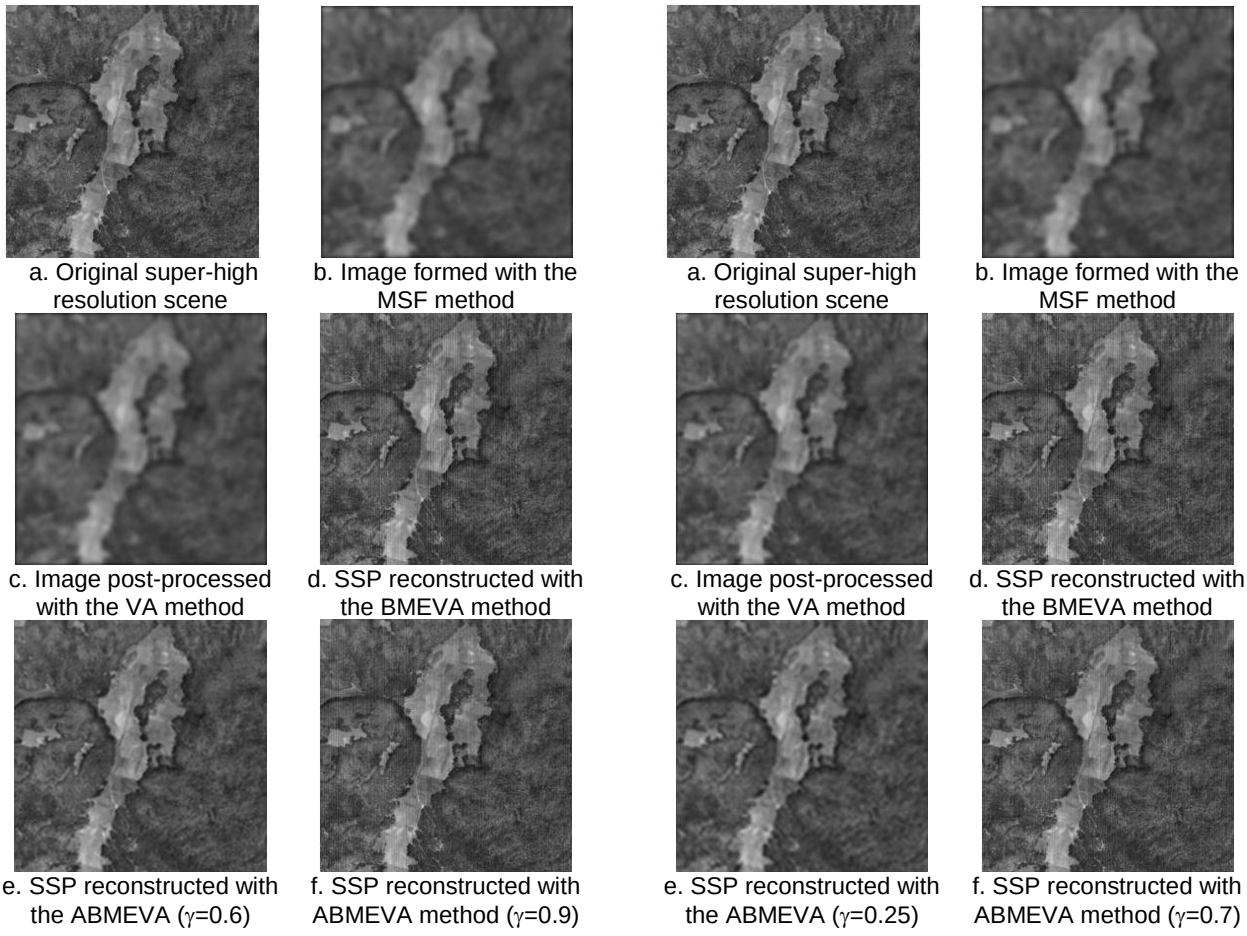

a. Original super-high resolution scene
b. Image formed with the MSF method
c. Image post-processed with the VA method
d. SSP reconstructed with the BMEVA method
e. SSP reconstructed with the ABMEVA (γ=0.6)
f. SSP reconstructed with ABMEVA method (γ=0.9)

Fig. 3. Simulation for **B'** scene (1st system model)

a. Original super-high resolution scene
b. Image formed with the MSF method
c. Image post-processed with the VA method
d. SSP reconstructed with the BMEVA method
e. SSP reconstructed with the ABMEVA (γ=0.25)
f. SSP reconstructed with ABMEVA method (γ=0.7)

Fig. 4. Simulation for **B'** scene (2nd system model)

Table 2. Scene **B'**-based results for two different simulated SAR systems

SNR [dB]	*IOSNR* [dB] System 1 Reconstruction Method				*IOSNR* [dB] System 2 Reconstruction Method			
μ	*VA*	*BMEVA*	*ABMEVA* (γ=0.6)	*ABMEVA* (γ=0.9)	*VA*	*BMEVA*	*ABMEVA* (γ=0.25)	*ABMEVA* (γ=0.7)
10	1.02	12.454	7.393	10.268	0.724	3.948	6.293	10.382
15	1.132	12.625	7.444	10.465	0.751	4.339	6.445	10.662
20	1.129	12.957	7.834	10.628	0.779	4.613	6.608	10.873
25	1.166	13.032	8.102	10.831	0.822	4.903	6.868	11.241
30	1.171	13.073	8.123	10.87	0.837	5.249	7.017	11.388

7 Concluding Remarks

The proposed approach termed ABMEVA presents a new iterative computational algorithm to improve the BMEVA performance. The key distinguishing feature of the ABMEVA method is the solution of image enhancement and denoising problem in the framework of a reference signal-based LMS algorithm that incorporates the spatial window operator (20) as input. This iterative reconstruction strategy produces better qualitative results than no-iterative strategies. A new adaptive computational algorithm provides sufficient qualitative evidence to discuss the ABMEVA computational efficiency. The ABMEVA offers a sub-optimal computational approach for the algorithm options, and it may be concluded that the proposed ABMEVA method demonstrates a substantially improved image enhancement and reconstruction in performing the adaptive windowing in flat regions while preserving the edge features.

The proposed ABMEVA manifests robust performance for different formation systems-based radar imaging.

References

1. **Black, M.J., Sapiro, G., Marimont, D.H., & Hegger, D. (1998).** Robust anisotropic diffusion. *IEEE Transaction on Image Processing*, 7(3), 421–432.
2. **Cichocki, A. & Amari, S. (2002).** *Adaptive blind signal and image processing.* Chichester; New York: John Wiley.
3. **Hamza, A.B., Krim, H. & Unal, G.B. (2002).** Unifying probabilistic and variational estimation. *IEEE Signal Processing Magazine*, 19(5), 37–47.
4. **Joshi, M. & Jalobeanu, A. (2010).** MAP estimation for multiresolution fusion in remotely sensed images using an IGMRF prior model. *IEEE Transactions on Geoscience and Remote Sensing*, 48(3), 1245–1255.
5. **Likas, A. & Galatsanos, N.P. (2007).** Bayesian methods based on variational approximations for blind image deconvolution. In P. Campisi & K. Egiazarian (Eds.), *Blind image deconvolution: Theory and applications* (141–168). Boca Raton: CRC Press.
6. **Martin, N. (2006).** Minimum variance. In F. Castanié (Ed.), *Spectral analysis: Parametric and non-parametric digital methods* (175–211), London; Newport Beach, CA: ISTE Ltd.
7. **Morales-Mendoza, L.J., Vazquez-Bautista, R.F. & Shkvarko, Y.V. (2005).** Unifying the maximum entropy and variational analysis regularization methods for reconstruction of the remote sensing imagery. *IEEE Latin America Transactions,* 3(4), 362–375.
8. **Nguyen, M. K. & Mohammad-Djafari, A. (1994).** Bayesian approach with the maximum entropy principle in image reconstruction from microwave scattered field data. *IEEE Transaction on Medical Imaging*, 13(2), 254-262.
9. **Plaza, A. & Chang, C. (2008).** High-performance computer architectures for remote sensing data analysis: overview and case study. In A. J. Plaza & C. Chang (Eds.), *High performance computing in*

remote sensing (9–41). Boca Raton: Chapman & Hall/CRC.

10. **Shkvarko, Y.V. (2002).** Estimation of wavefield power distribution in the remotely sensed environment: Bayesian maximum entropy approach. *IEEE Transactions on Signal Processing,* 50(9), 2333–2346.
11. **Shkvarko, Y.V. (2004).** Unifying regularization and Bayesian estimation methods for enhanced imaging with remotely sensed data-part I: Theory. *IEEE Transactions on Geoscience and Remote Sensing*. 42(5), 923–931.
12. **Solberg, A.H.S. (2007).** Data fusion for remote sensing applications. In C.H. Chen (Ed.), *Signal and image processing for remote sensing* (515–537).Boca Raton: CRC/Taylor & Francis.
13. **Vázquez-Bautista, R. F., Shkvarko, Y.V. & Morales-Mendoza, L.J. (2003).** Aggregating the statistical estimation and variational analysis methods in radar imagery. *2003 IEEE International Geoscience and Remote Sensing Symposium (IGARSS'03),* Toulouse, France, 3, 2008–2010.
14. **Vázquez-Bautista, R.F., Morales-Mendoza, L.J., Ortega-Almanza, R. & Blanco-Ortega, A. (2010).** Adaptive algorithm-based fused Bayesian maximum entropy-variational analysis methods for enhanced radar imaging. *Advances in Pattern Recognition*. *Lectures Notes in Computer Science,* 6256, 154–163.

René F. Vazquez Bautista received the B.S. degree in Electronics and Communications Engineering from Veracruzana University; the M. Eng. in Electrical Engineering from Guanajuato University; and Ph.D. degree by CINVESTAV, Guadalajara in 2000, 2002 and 2006, respectively. From 2007 to 2009, he had been with the ITESM, Campus Guadalajara as an assistant Professor. Nowadays, He is a Veracruzana University´s full Professor in FIEC, Campus Poza Rica. His research interests are Digital Signal and Image Processing, Data and Sensor Fusion, Biomedical Applications and Embedded Systems.

Andrés Blanco Ortega graduated in Electromechanic Engineering from the Instituto Tecnológico de Zacatepec in 1993. He received a MSc. Degree in Mechanical Engineering from Centro Nacional de Investigación y Desarrollo Tecnológico in 2001, and a Ph.D. in Electric Engineering from the CINVESTAV-IPN in Mexico, in 2004. He is a full professor at CENIDET. His interests are active vibration control and mechatronic design, specifically, rotating machinery.

Luis J. Morales Mendoza was born in Veracruz, Mexico in 1974. He received a B.S. degree in Electronics and Communications Engineering from Veracruzana University in 2001, a M.S. degree in Electrical Engineering from the Guanajuato University, Mexico, 2002, and a Ph.D. degree in Electrical Engineering from CINVESTAV, Guadalajara in 2006. From 2006 to 2009, he worked at the Electronics Department of the Guanajuato University of Mexico as an Assistant Professor. He is currently a Professor of the FIEC of the Veracruz University of Mexico. His scientific interests are artificial neural networks applied to optimization problems, image restoration and enhancing, and ultrasound image processing. He is the author and the co-author of more than 40 journal and conference papers.

Francisco Beltrán Carbajal is with Universidad Politécnica de la Zona Metropolitana de Jalisco. He obtained his Electromechanical Engineer degree in 1993 from the Instituto Tecnológico de Zacatepec (México) and Ph.D. degree in Electrical Engineering in 2004 from the Centro de Investigación y Estudios Avanzados del Instituto Politécnico Nacional (CINVESTAV-IPN), Mexico City. His research interests are active vibration control of mechanical systems and mechatronic design.

Article received on 11/19/2010; accepted 05/05/2011.